Effects of Shaft Grouting on the Bearing Behavior of Barrette Piles: A Case Study in Ho Chi Minh City

Phu-Huan Vo Nguyen
Infrastructural Technique Department
Faculty of Civil Engineering
Ho Chi Minh City Open University
Ho Chi Minh City, Vietnam
huan.vnp@ou.edu.vn

Phu-Cuong Nguyen
Advanced Structural Engineering Laboratory
Structural Engineering Department
Faculty of Civil Engineering
Ho Chi Minh City Open University
Ho Chi Minh City, Vietnam
cuong.pn@ou.edu.vn

Abstract—The shaft-grouted method has been applied on high-rise buildings in Ho Chi Minh City for the purpose of increasing the bearing capacity of barrette piles. The Exim Bank Building foundation, using two kinds of shaft-grouted barrette piles, was 65m (TP1) and 85m (TP2) in depth. To assess the bearing capacity, this project assembly used the O-cell tools installed at 49m depth below the pile head level. Shaft grouting was performed from -25m to the TP1 pile toe level and -65m to the TP2 pile toe level. This work is based on the data from the O-cell experiments at the construction site and the results of finite element simulation in Plaxis software. The effectiveness of shaft grouting was analyzed and the length and position of the ejector were evaluated and compared in order to find the best solution for applying shaft grouting with the aim to ensure safety and mitigate economic problems.

Keywords-bearing capacity; barrette pile; shaft grouting; O-cell test; Plaxis

I. INTRODUCTION

High-rise building foundations in Ho Chi Minh City are constructed by using bored piles and barrette piles to ensure the total loads of structures. The shaft resistance using the grouting method has been reported in [1-3, 7, 8, 11]. Authors in [7] carried out laboratory tests in sand to find the behavior of density, soil gradation, and stress on the shaft resistance in grouting methods. The increase of shaft resistance was indicated by the low mobility grout. Authors in [2, 3] studied the bored piles in Ho Chi Minh City. In the results, the shaft resistance development in bored piles gains maximum resistance after a movement of only 3mm to 4mm. The Osterberg test (O-cell test) in principle is exactly the same as the static compression test, and it is dedicated to bored piles and barrettes. The testing principle is to apply the load directly on the pile tip or the pile body using a device called Osterberg cell. It is quite possible to use the pile load, the lateral soil friction, and the tip resistance as counterweights to increase the load. The Osterberg test method will give a result in which the two curves of load and displacement at the pile tip and pile head are built independently. The purpose of this paper is to evaluate the effectiveness of shaft grouting method on the barrette piles in Ho Chi Minh City and compare it with the no shaft-grouted method in order to find the best position to install the ejector using the Finite Element Method (FEM).

II. PROJECT INFORMATION

The Eximbank building is located at District 1, Ho Chi Minh City. It consists of 5 basements and 40 storys with a construction area of 3518m^2. Its design adopts 2 barrette test piles of 2800×800mm size and 15MN load [3]. The TP1 pile is 65.3m in depth near the borehole no. 2. The TP2 pile is 85.3m in depth near the borehole no. 8. Their designed to be grouted lengths are 40m for TP1 and 21m for TP2 respectively from their upward tips. The geological survey report states the soil condition at the test piles as follows: soft clay stratum at a depth of 7m, sandy stratum at the tips at 41m, mixed clay at 52m and finally a dense and very dense sandy stratum. O-Cell hydraulic jack is installed 16m from the pile tip and strainometers are installed along its body as shown in Figure 4 of [3]. Figure 1 shows how to install the equipment on the cross-sectional area of the two piles in which the main 32-dia steel bar of each pile is joined with the loop reinforcement to its frame. The total main steel bar area of the pile is 289cm^2 and the pile cross-sectional area is 2.24m^2. The grout pipe with a diameter of 60mm is mounted around the perimeter of the steel frame throughout the length of the pile and 39.7m and 21.2m lower than the lengths of TP1 and TP2 respectively. The grout pipe must be perforated to allow the grout to escape and it can be capped to ensure a secure grouting.

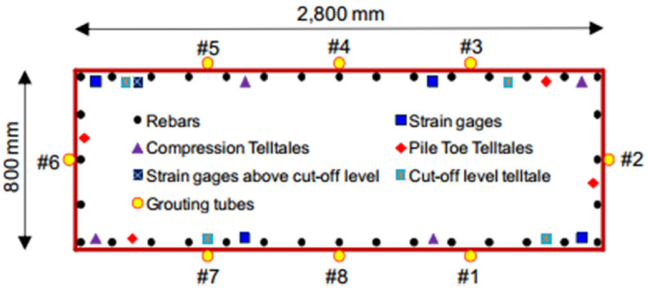

Fig. 1. Cross section and details of installation equipment for piles.

Corresponding author: Phu-Huan Vo Nguyen

III. PILE LOAD-BEARING ANALYSIS

A. Test Results in Site

The results of the force-displacement relationship curve of the O-cell test performed on the two test piles TP1 and TP2 can be seen in Figure 7 of [3]. The force acting on the O-cell is evaluated and adjusted subjecting to the pile self-load and the water pressure at the depth of the O-cell placement. After the duration of holding the maximum load is over, the displacement values of the lower O-cell are 9.0mm and 5.9mm, and the pile tip displacement values are 4.6mm and 2.2mm respectively. The displacement values of the upper O-cell are 6.7mm and 6.9mm and the pile end displacement values are 1.2mm and 0.8mm.

B. FEM Analysis

The determination of the input data for the model is made on the basis of the correlation equations and empirical researches [9, 12-14] as follows:

- The Young's modulus, E_{50ref}, is determined from the drained 3-dimensional (3-D) consolidation test with the selected chamber pressure level σ_3 in accordance with the actual state of the soil profile.
- Drained shear strength parameters are taken from the drained 3-dimensional consolidation test or as the effective shear strength values in the undrained 3-D consolidation test. For the soil profile without the 3-D CU test, CD can be obtained from the direct shear strength test, but its reliability is not high. The undrained shear strength parameter also does not take the friction angle of the ground soil, $\varphi_u = 0$, into account but only the adhesion force of the soil C_u. C_u values are obtained through the undrained 3-D test, the in-situ shear vane test, or the 1-dimensional unconfined compressive test.
- For dense layers of sand or over-consolidated layers of clay, the expansion angle ψ exists. Normally, according to the instructions of Plaxis software, $\psi = \varphi - 30^0$. In other cases, the expansion angle is equal to 0.

The parameters of the Hardening Soil model are determined directly from the geological survey report test results or from the correlation equations of the previous researches to obtain the values summarized in Table I.

TABLE I. SOIL PARAMETERS IN FEM

No.	Backfill	Layer 1	Layer 2	Layer 3	Layer 3b	Layer 4	Layer 6
Type	HS	HS	HS	HS	HS	HS	HS
γ_{unsat} (kN/m^3)	18.56	14.61	18.42	18.35	19.23	20.38	19.93
γ_{sat} (kN/m^3)	18.80	15.59	19.31	19.21	19.94	20.66	20.62
E^{ref}_{50} (kN/m^2)	11210	4000	18000	60000	80000	95000	90000
E^{ref}_{oed} (kN/m^2)	11210	4000	18000	60000	80000	95000	90000
E^{ref}_{ur} (kN/m^2)	56030	20000	90000	250000	370000	350000	330000
m	0.75	1	0.85	0.5	0.5	0.75	0.6
v_{ur}	0.2	0.2	0.2	0.2	0.2	0.2	0.2
c (kN/m^2)	22.41	13.77	36	4.1	4.1	218.4	1.7
$\varphi^{(o)}$	0	0	4.8	32.49	32.49	0	37.00
$\psi^{(o)}$	0	0	0	2.49	2.49	0	7.00
R_{inter}	0.85	0.7	0.7	0.85	0.85	0.85	0.85

To make load capacity comparison easier, the 4 used models in Plaxis 2D software were:

- Model 1: TP1 pile with grouting
- Model 2: TP1 pile without grouting.
- Model 3: TP1 pile with grouting only from -26.3m to -48.5m.
- Model 4: TP1 pile with grouting only from -48.5m to -65.5m.

Firstly, the TP1 pile with grouting will be simulated, because it is most similar to the actual observation. After obtaining its results (note that the load level is gradually adjusted until failure) the parameters change. Pile TP1 becomes a non-grouted pile, and also from that model, the set of parameters change in order to simulate the models 3 and 4 (the grouting length from -26.3m to -48.5m and -48.5m to -65.5m respectively). The obtained results are used to draw the relationship graph of the curve and the load of the four investigated models. We convert the test load of the Osterberg method into the conventional static test load using an equivalent method, from which we have enough basis to evaluate the increase in the load capacity of the TP1 pile according to the four different models.

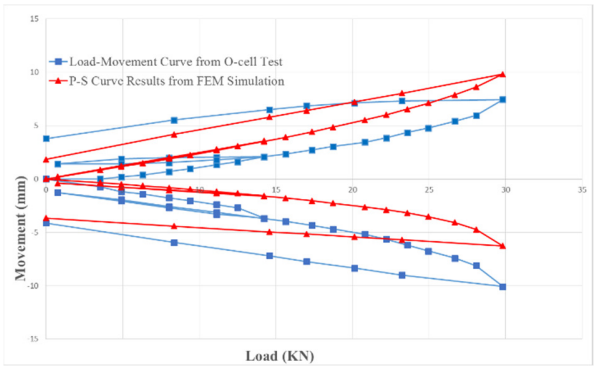

Fig. 2. Movement and load curves obtained from actual and simulated observations.

The O-cell upper displacement is 7.44mm/9.82mm on site. The O-cell lower displacement is -10.08mm/-6.27mm on site. The total strain of the O-cell is 17.52/16.09mm. This result from Figure 2 shows that the measured results and the finite element modeling have high accuracy. However, in terms of displacement between the upper and lower O-cells, there is an inversion. The field displacement value is smaller than that of the Plaxis model, i.e. 7.44/9.82mm. It should be noted that the lateral friction is enhanced due to the better grouting ability (regarding the safety issue). For the lower O-cell, in fact, the tip resistance has not been applied to the load-carrying capacity of the pile, so the actual displacement is larger than that of the Plaxis model -10.08/-6.27mm).

IV. DISSCUSION

This analytical model is rather similar to the investigated field, so the authors take this set of soil parameters to continue to simulate the remaining models with the condition of

increasing load until the failure of the pile. The results of models 1-4 are displayed in Figures 3-6.

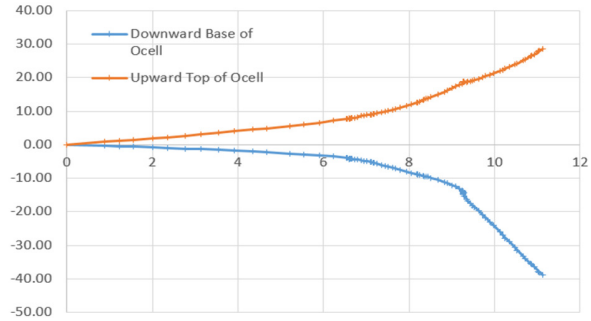

Fig. 3. Model 1. The TP1 pile with grout reaches 305% of maximum load.

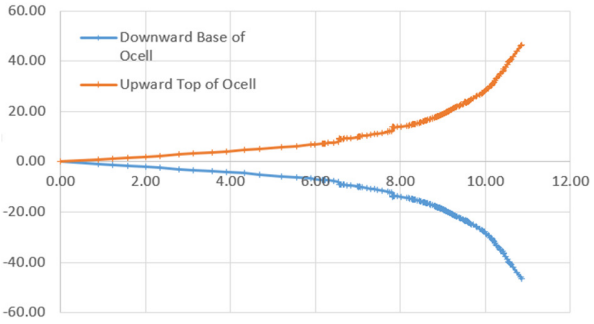

Fig. 4. Model 2. The TP1 pile without grout reaches 255% of maximum load.

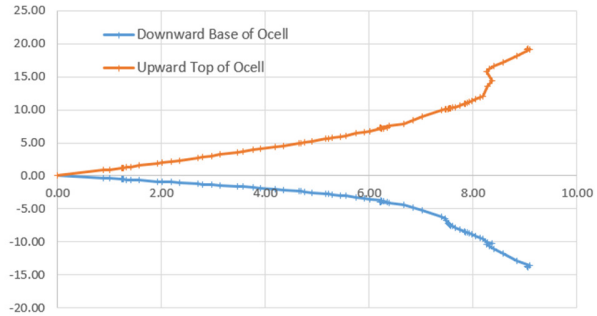

Fig. 5. Model 3. The TP1 pile with grout from -26.3m to -48.5m reaches 280% of maximum load.

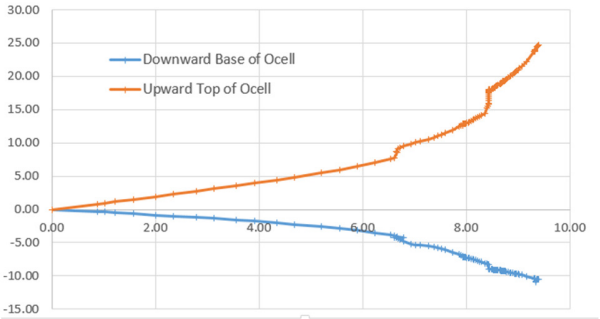

Fig. 6. Model 4. The TP1 with grout from -48.5m to -65.5m reaches 280% of maximum load

The ultimate load capacity is determined based on the shape of the load-displacement relationship curve:

$$S = f(P), \log S = f(\log P) \quad (1)$$

In many cases, it is necessary to combine with other curves like:

$$S = f(\log t), P = f(S/\log t) \quad (2)$$

With the load-displacement relationship curve, the ultimate load-carrying capacity is determined as follows:

- Case 1: the P-S relationship curve has a clear bending point. The ultimate load-carrying capacity is determined directly on the curve, the load corresponding to the point where the curve begins to change suddenly or the curve is closely parallel to the displacement axis.
- Case 2: the P-S relationship curve changes slowly. It is quite difficult or impossible to accurately determine the bending point. The ultimate load-carrying capacity is determined by different graphical methods.

The analysis and evaluation of the test results by the Osterberg method are still based on the principles of conventional static testing, in which the Q-S relationship curve is an important tool of the quantitative analysis of the load-carrying capacity of the piles that a mechanical problem usually covers. The goal of load testing in most cases is not only to determine the bearing capacity of the pile foundation, but also to get a more specific view than the one from the general theory and the calculated results about the interaction between the pile and the composing ground so that we can offer more appropriate behaviors in the design of the pile foundation and in the future construction processing. We can build a load-settlement curve (similar to a conventional static compression test curve) in the following way:

At any displacement S, the downward force affecting the soil is:

$$Q'\downarrow = Q\downarrow + w_2' \quad (3)$$

where $Q\downarrow$ is the downward force by the O-cell at the displacement S and w_2 is the self-load of the pile from the O-cell downwards (buoyancy must be taken into account if we are below the groundwater level).

At the same displacement S, the upward force carried by the soil is:

$$Q'\downarrow = (Q\downarrow - w_1') \times F \quad (4)$$

where w_1' is the self-load of the pile from the O-cell upwards (buoyancy must be taken into account if we are below the groundwater level) and F is the coefficient that takes into account the difference in the lateral friction between the normal static compression and the Osterberg compression. With F = 1.00 for the pile in the rock and F = 0.95 for the pile in the loose soil.

At the displacement S, the sum of the upward and downward forces will be subjected by the soil:

$$P = Q'\downarrow + Q'\downarrow = Q\downarrow + w2' + (Q\downarrow - w1') \times F \quad (5)$$

However, in the case of downward compression, the soil is already partially imposed by the self-load of the pile, so the applied load at the top of the pile is:

$$P_e = P - w_1' - w_2' = Q\downarrow + (Q\downarrow - w_1') \times F - w_1' \quad (6)$$

At a load of P_e (loading downwards), the settlement of the pile is $S + \Delta\delta$ where the increment $\Delta\delta$ refers to the elastic compressive strain of the pile.

Repeating the above steps with different positions S, we can draw a static compression curve corresponding to the data pair (P_e, $S + \Delta\delta$). If at a certain position that goes beyond the range of a curve (for example, the lateral resistance curve of the pile segment on the jack), we choose one of the following two solutions:

- Take the upward force as constant (regarded as the extreme value) and equal to the tested maximum lateral resistance.
- Extrapolating the next segment of the lateral resistance curve. However, this extrapolation has errors, because if the pile body is very rough (convex), then the lateral resistance reaches its ultimate value more slowly. Conversely, the less convex and concave the pile body is, the faster the lateral resistance reaches its ultimate value.

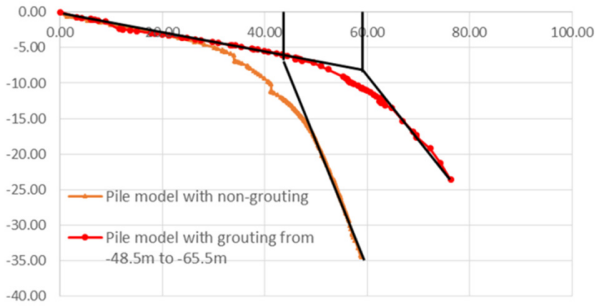

Fig. 7. Load capacity of the pile in the models 2 and 4.

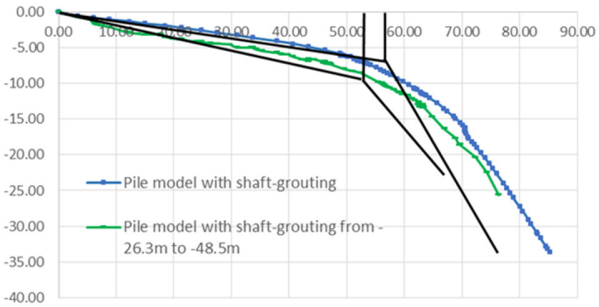

Fig. 8. Load capacity of the pile in the models 1 and 3.

From the above analysis, we will convert equivalently the test results of the Osterberg method into those of the conventional test method to plot the P-S relationship curve from the data pair (P_e, $S + \Delta\delta$) and then use the graphical method to determine the load capacity. The results of the shape of the load-displacement relationship curve are displayed in Figures 7-9.

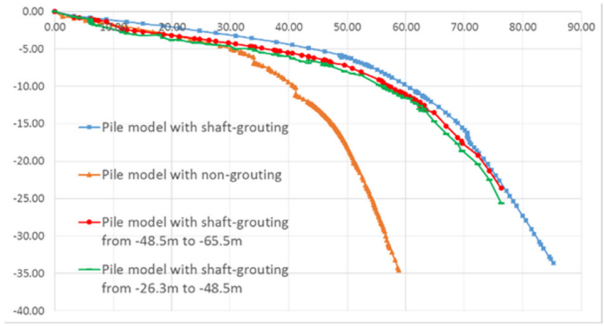

Fig. 9. Summary of the pile load-carrying capacity of the 4 models.

V. CONCLUSION

Through the experimental study from the O-cells of the TP1 pile in the Eximbank building on the ability to improve the load-carrying capacity of the lateral walls, the following conclusions can be drawn:

- Improvement of the bearing capacity of the pile by the lateral grouting method is highly effective with results of 61.7MN and 41.8MN with and without grout respectively. The friction performance of the pile body with grouting increases by 1.48 times. It is different from the previous studies that we compared the analytical equations and the field results.
- Grouting of each segment at depths of 22.2m (from -26.3m to -48.5m) and 16.8m (from -48.5m to -65.3m) corresponding to the maximum load of 59.2MN and 59.4MN is evaluated as being similar to the load-carrying capacity. The FEM simulation results show that the bigger grouting length and the bigger grouting depth will give higher values of bearing capacity. Simulating grouting in each segment is very beneficial for the design of allowable loads, both in terms of safety and cost aspects.
- The FEM (Plaxis) can simulate and evaluate the O-cell and the lateral grouting tests of piles. This method can be used for computational correction after the field results are available for detailed design.

ACKNOWLEDGMENT

The current research is supported by the Ho Chi Minh City Open University (Project No. E2019.08.3).

REFERENCES

[1] B. H. Fellenius, "Tangent Modulus of Piles Determined from Strain Data," presented at the Foundation Engineering: Current Principles and Practices, 1989, pp. 500–510.

[2] B. H. Fellenius, "Analysis of results of an instrumented bidirectional-cell test," *Geotechnical Engineering Journal of the SEAGS & AGSSEA*, vol. 46, no. 2, pp. 64–67, 2015.

[3] H. M. Nguyen, B. H. Fellenius, A. J. Puppala, P. Aravind, and Q. T. Tran, "Bidirectional Tests on Two Shaft-Grouted Barrette Piles in Mekong Delta, Vietnam," *Geotechnical Engineering Journal of the SEAGS & AGSSEA*, vol. 47, no. 1, pp. 15–25, Mar. 2016.

[4] L. M. Zhang and L. F. Chu, "Calibration of Methods For Designing Large-Diameter Bored Piles: Ultimate Limit State," *Soils and Foundations*, vol. 49, no. 6, pp. 883–895, Dec. 2009, https://doi.org/10.3208/sandf.49.883.

[5] "Report on Barrtte load testing TP2- Eximbank Tower, Ho Chi Minh City, Viet Nam," 138131–2, Sep. 2013.

[6] "Pile Foundation - Design Standard," National Standards, VN 10304: 2014.

[7] S. Pooranampillai, S. Elfass, W. Vanderpool, and G. Norris, "Large Scale Laboratory Testing of Low Mobility Compaction Grouts for Drilled Shaft Tips," *Geotechnical Testing Journal*, vol. 33, no. 5, pp. 397–409, Sep. 2010, https://doi.org/10.1520/GTJ102658.

[8] G. D. Plumbridge, B. D. Littlechild, S. J. Hill, and M. Pratt, "Full-scale shaft grouted piles and barrettes in Hong Kong–A First," in *Proceedings of the Nineteen Annual Seminar of the Geotechnical Division of the Hong Kong Institution of Engineers*, Hong Kong, China, 2000, pp. 159–166.

[9] T. Nguyen, V. Q. Lai, D. L. Phung, and T. P. Phan, "Shaft Resistance of Shaft-grouted Bored Piles and Barrettes Recently Constructed in Ho Chi Minh City," *Geotechnical Engineering*, vol. Vol. 50, no. 3, pp. 155–162, Sep. 2019.

[10] J. Zhou, X. Gong, and R. Zhang, "Model tests comparing the behavior of pre-bored grouted planted piles and a wished-in-place concrete pile in dense sand," *Soils and Foundations*, vol. 59, no. 1, pp. 84–96, Feb. 2019, https://doi.org/10.1016/j.sandf.2018.09.003.

[11] X. Zhao, G. Zhou, G. Zhao, L. Kuang, and X. Hu, "Fracture controlling of vertical shaft lining using grouting into neighboring soil deposits: A case study," *Soils and Foundations*, vol. 57, no. 5, pp. 882–891, Oct. 2017, https://doi.org/10.1016/j.sandf.2017.08.018.

[12] N. Mangi, D. K. Bangwar, H. Karira, S. Kalhoro, and G. R. Siddiqui, "Parametric Study of Pile Response to Side-by-Side Twin Tunneling in Stiff Clay," *Engineering, Technology & Applied Science Research*, vol. 10, no. 2, pp. 5361–5366, Apr. 2020, https://doi.org/10.48084/etasr.3290.

[13] T. A. Rind, H. Karira, A. A. Jhatial, S. Sohu, and A. R. Sandhu, "Particle Crushing Effect on The Geotechnical Properties of Soil," *Engineering, Technology & Applied Science Research*, vol. 9, no. 3, pp. 4131–4135, Jun. 2019, https://doi.org/10.48084/etasr.2730.

[14] A. H. Bhutto *et al.*, "Mohr-Coulomb and Hardening Soil Model Comparison of the Settlement of an Embankment Dam," *Engineering, Technology & Applied Science Research*, vol. 9, no. 5, pp. 4654–4658, Oct. 2019, https://doi.org/10.48084/etasr.3034.